

Optical Engineering

OpticalEngineering.SPIEDigitalLibrary.org

Effects of mitigation of pixel cross-talk in the encoding of complex fields using the double-phase method

Miguel Carbonell-Leal
Omel Mendoza-Yero

SPIE.

Miguel Carbonell-Leal, Omel Mendoza-Yero, "Effects of mitigation of pixel cross-talk in the encoding of complex fields using the double-phase method," *Opt. Eng.* **59**(4), 041203 (2019), doi: 10.1117/1.OE.59.4.041203.

Effects of mitigation of pixel cross-talk in the encoding of complex fields using the double-phase method

Miguel Carbonell-Leal and Omel Mendoza-Yero*

Institut de Noves Tecnologies de la Imatge (INIT), Universitat Jaume I, Castelló, Spain

Abstract. We report on unwanted effects of pixel cross-talk and its mitigation on the experimental realization of the double-phase method with phase-only spatial light modulators. We experimentally demonstrate that a generalized sampling scheme can reduce nonuniform phase modulation due to the pixel cross-talk phenomenon and, consequently, improve the quality of amplitude and phase images obtained with this encoding method. To corroborate our proposal, several experiments to reconstruct amplitude-only as well as fully independent amplitude and phase patterns under different spatial sampling schemes were carried out. We also show how a convenient implementation of the well-known polarization-based phase-shifting technique can be employed to measure the encoded complex field using only a conventional CMOS camera. © The Authors. Published by SPIE under a Creative Commons Attribution 4.0 Unported License. Distribution or reproduction of this work in whole or in part requires full attribution of the original publication, including its DOI. [DOI: [10.1117/1.OE.59.4.041203](https://doi.org/10.1117/1.OE.59.4.041203)]

Keywords: diffractive optics; beam shaping; phase modulation; interferometry; liquid crystal devices; pixel cross-talk.

Paper 191016SS received Jul. 26, 2019; accepted for publication Oct. 22, 2019; published online Nov. 21, 2019.

1 Introduction

At present, there is a wide variety of reported optical methods to optically manipulate the complex field of laser beams using spatial light modulators (SLMs).^{1–14} Among them, those based on the use of parallel-aligned liquid crystal on silicon (PA-LCoS) SLMs have gained special attention not only because of their relative high efficiency but also due to their proven ability to accurately modify the physical behavior of laser beams using just a single-phase element encoded into a phase-only SLM.^{3,4,7,8–14} In this context, among many other applications and/or signal-displaying methods, computer-generated holograms have been synthesized by means of conventional iterative Fourier transform algorithms,¹⁵ employing a search, also iterative, algorithm capable of generating binary holograms;¹⁶ using a complex amplitude modulation method for three-dimensional dynamic holographic display;¹⁷ by the application of the one-step phase-retrieval approach, which allows a rapid computation of phase-only holograms;¹⁸ by downsampling the intensity image with uniform grid-cross lattices;¹⁹ or more recently by adding a periodic phase pattern to the source image.²⁰ Here, we deal with a particular interferometric method²¹ aimed at encoding and retrieving the complex field of coherent laser beams. This method has been widely and successfully employed in several experimental tasks, including but not limited to demonstrating the Talbot self-imaging in the azimuthal angle,²² generating speckleless holographic displays,²³ trapping magnetic microparticles employing Bessel-Gauss beams,²⁴ shaping optical vector beams,²⁵ or experimentally investigating the propagation and focusing characteristics of Airy beams.^{26,27} In all of these applications, the implementation of the above-mentioned encoding method²¹ was carried out with the help of a commercially available PA-LCoS SLM. So, light undergoes phase modulation due to a change in the refractive index

of the nematic liquid crystal (LC) material. Specifically, the phase shift is associated with the tilt of the SLM molecules when a signal voltage is applied between the front and the back faces of each LC cell. In addition, the main design features of these devices ensure, in principle, that the phase modulation process is done with almost no coupling of amplitude modulation or change in the polarization state of the incident light, which is highly desirable for applications involving interference or diffraction phenomena.

However, PA-LCoS SLMs are not ideal devices as they show some effects that cause degradation of the phase modulation. For instance, temporal fluctuations of the LC molecular orientation as a function of time causes depolarization effects, deteriorating the diffraction efficiency of SLM.²⁸ Another harmful effect is related to the Fabry–Perot multiple beam interference generated by the intrinsic layer structure of the LC device²⁹ that may originate nonlinear phase modulation or even some coupling of amplitude modulation. In this context, there is a particular unwanted effect that becomes critical for applications that require encoded patterns with abrupt phase discontinuities, e.g., diffraction gratings with few phase levels or phase distributions associated with high scattering media. In the literature, this widely studied phenomenon,^{30–33} known as the fringing field effect (or pixel cross-talk effect), can produce variations in the orientation of LC molecules at adjacent cells and consequently modify its expected phase response. Hence, as in the double-phase method,²¹ the encoded element is generated by the spatial multiplexing of two-phase patterns at the Nyquist limit; one might expect that its experimental realization with PA-LCoS SLMs does not lack from pixel cross-talk effects.

In this study, we experimentally show that pixel cross-talk effects do deteriorate the amplitude and phase patterns obtained due to the application of the double-phase method.²¹ To alleviate these problems, a generalized sampling scheme that is able to significantly reduce nonuniform phase modulation without compromising the accuracy of the method is proposed. To avoid the influence of the zero order coming

*Address all correspondence to Omel Mendoza-Yero, E-mail: omendoza@fca.uji.es

from the SLM on the measurements done throughout this work, a fixed blazed grating was added to each phase element sent to the SLM, in the same manner as proposed in Ref. 23.

2 Fundamentals of the Proposal

The theory underlying the double-phase method²¹ can be briefly described as follows. Any complex field represented in the form $U(x, y) = A(x, y)e^{i\varphi(x, y)}$ can also be written as

$$U(x, y) = e^{i\theta(x, y)} + e^{i\vartheta(x, y)}, \quad (1)$$

where

$$\theta(x, y) = \varphi(x, y) + \cos^{-1}[A(x, y)/A_{\max}], \quad (2)$$

$$\vartheta(x, y) = \varphi(x, y) - \cos^{-1}[A(x, y)/A_{\max}]. \quad (3)$$

In Eqs. (1)–(3), the amplitude and phase of the two-dimensional complex field $U(x, y)$ is given as $A(x, y)$ and $\varphi(x, y)$, respectively. In addition, $A_{\max} \equiv 2$ holds for the maximum of $A(x, y)$. From Eq. (1), it is apparent that $U(x, y)$ can be obtained from the coherent sum of the uniform waves $e^{i\theta(x, y)}$ and $e^{i\vartheta(x, y)}$. To do that using just a phase-only SLM, the above uniform waves are spatially multiplexed with two-dimensional complementary binary gratings (see Fig. 1). This allows us to get a single-phase element $\alpha(x, y)$ as follows:

$$M_1(x, y)e^{i\theta(x, y)} + M_2(x, y)e^{i\vartheta(x, y)} = e^{i\alpha(x, y)}, \quad (4)$$

where

$$\alpha(x, y) \equiv M_1(x, y)\theta(x, y) + M_2(x, y)\vartheta(x, y). \quad (5)$$

At this point, the interference of the above-mentioned uniform waves cannot happen if we do not mix the information contained in the phase element $\alpha(x, y)$. This is carried out using a spatial filter that is capable of blocking all diffraction orders but the zero one. Here, it should be mentioned that, for the off-axis setup employed in this work, the filtering process is done around the order at which the blazed grating achieves its maximum diffraction efficiency.

It can be shown that, after this filtering process, the spectrum of the original complex field at the Fourier plane can be exactly retrieved. Consequently, at the output plane of

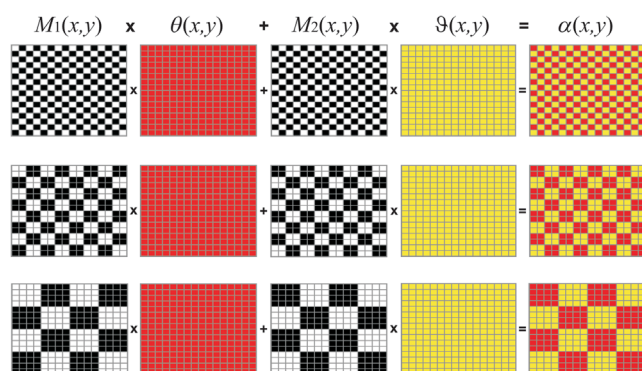


Fig. 1 Examples of the design process of trivial phase elements $\alpha(x, y)$ obtained with sampling gratings having pixel-cells of 1×1 , 2×2 , and 4×4 pixels, respectively.

the imaging system, the retrieved complex field $U_{\text{RET}}(x, y)$ (without considering constant factors) is given as the convolution of the magnified and spatially reversed complex field $U(x, y)$ with the Fourier transform of the filter mask, that is

$$U_{\text{RET}}(x, y) = U(-x/\text{Mag}, -y/\text{Mag}) \otimes F\{P(u, v)\}. \quad (6)$$

In Eq. (6), the convolution and Fourier transform operations are denoted by the symbols \otimes and $F\{\}$, respectively. In addition, the term Mag represents the magnification of the imaging system, whereas $P(u, v)$ is the filter function with coordinates u and v in the frequency space. So, from Eq. (6), in theory, the amplitude and phase of the original complex field is fully retrieved, except for some loss of spatial resolution due to the convolution operation.

In practice, the real physical behavior of phase-only SLM devices under extreme pixel-to-pixel phase modulation conditions can originate discrepancies between the theory and the experiment. This mainly happens because the phase information associated with each uniform wave is spatially multiplexed at the Nyquist limit. However, if the period of the binary gratings is not taken at the Nyquist limit, but the spatial frequency separations of diffraction orders are great enough to avoid overlapping among them, the Whittaker–Shannon sampling theorem ensures that, for bandlimited functions, the reconstruction of the spectrum at the Fourier plane is still accomplished exactly. Hence, the utilization of phase elements $\alpha(x, y)$ computer-generated from binary gratings with more than 1 pixel/cell should alleviate unwanted cross-talk effects.

3 Experimental Corroboration of the Proposal

To show the effects of pixel cross-talk on the retrieved complex field and how to mitigate them, we carry out two experiments. The optical setup used for both experiments is shown in Fig. 2. As a light source, we use a quasi-monochromatic laser beam of 10-nm spectral width and centered at 800 nm. Before it impinges onto a reflective phase-only PA-LCoS SLM (Holoeye Pluto optimized for 700 to 1000 nm, resolution 1920×1080 pixels, pixel pitch $8 \mu\text{m}$, and phase range 3π), the beam is conveniently attenuated with neutral filters and spatially magnified using a commercial reflective $6\times$ beam expander (Thorlabs BE06R). Then, the beam is sent to the SLM, forming a small angle with the normal to the LC surface of about 4° , and is back-reflected toward the entrance of a $4f$ imaging system. The input plane of this optical system coincides with the SLM plane. The $4f$ imaging system is made up of two refractive lenses (L_1 and L_2) with focal lengths of 1 and 0.5 m, respectively. This pair of lenses gives a transversal demagnification of $1/2$ at the output plane of the imaging system. This reduction allows us to directly

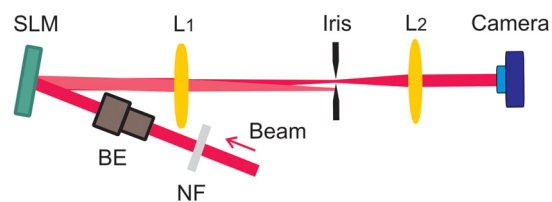


Fig. 2 Off-axis optical setup used to investigate the effects of pixel cross-talk in double-phase method. Acronyms of included elements are NF (neutral filters), BE (beam expander), SLM (spatial light modulator), and L_1 and L_2 (refractive lenses).

measure the irradiances with a CMOS camera (Ueye UI-1540M, 1280×1024 pixel resolution, and 5.2 pixel pitch). Nondiffracted light was removed from the setup using a blazed grating having a fixed period of $p = 160 \mu\text{m}$ and encoded from $-\pi$ to π with 20 phase levels per period. At the Fourier plane, the beam is transmitted through a low-pass spatial filter that consists of a hard circular iris (Thorlabs ID 12Z/M). The iris size was adjusted each time to fulfill the filtering condition.

In the first experiment, an amplitude-only pattern given by a mushroom image is encoded with the double-phase method²¹ into the SLM using three different sampling gratings. This encoding process is exemplified in Fig. 1 with a trivial case. For this experiment, we employ binary gratings of 1×1 , 4×4 , and 10×10 pixels/cell. The measured amplitude images are shown in Fig. 3.

If we compare the original image given in Fig. 3(a) with the remaining ones, it is clear that image quality is affected by the nonuniform phase response of the SLM. At the Nyquist limit [see Fig. 3(b)], the recorded image has the best resolution, but its brightness is so high that contrast becomes really poor. When pixel-cell size is increased up to 16 pixels/cell, the image contrast and sharpness are greatly improved at the expense of a slight decrease of resolution [see Fig. 3(c)]. This can be regarded as an optimal situation because cross-talk effects are mitigated and image resolution is still acceptable. However, if pixel-cell size is increased too much, like in Fig. 3(d) with 100 pixels/cell, problems relating to the loss of resolution predominate over any potential improvement in the image quality.

In the second experiment, we use the double-phase method²¹ to reconstruct a nontrivial complex field under the sampling configuration of 1×1 , 2×2 , and 5×5 pixels/cell. In this case, a convenient implementation of the polarization-based phase-shifting technique³⁴ is applied to measure the retrieved complex field. This implementation can be explained by the following three steps. In the first one, after multiplying the phase element $\alpha(x, y)$ by an additional two-dimensional binary grating $M_3(x, y)$, some pixel-cells of $\alpha(x, y)$ are periodically eliminated. Particularly, $M_3(x, y)$ has double the period of $M_1(x, y)$ or $M_2(x, y)$. In Fig. 4, this first step is shown by two examples corresponding to trivial cases given in Fig. 1.

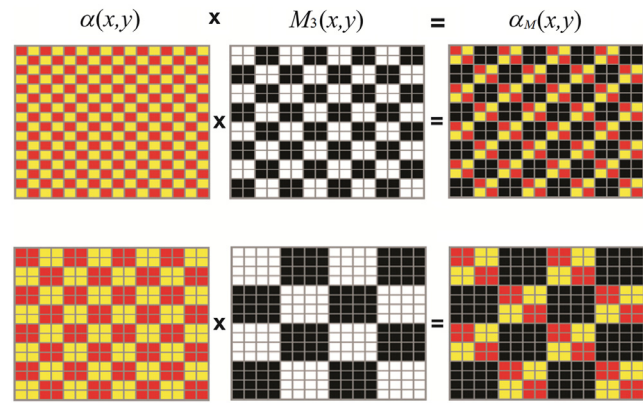


Fig. 4 Examples of two modified phase elements $\alpha_M(x, y)$ obtained after a convenient sampling process with a binary grating $M_3(x, y)$.

In the second step, the blazed grating is added to the modified phase element $\alpha_M(x, y)$. Finally, in the last step, the interferograms are determined with the help of four uniform phases with values of 0 , $\pi/2$, π , and $3\pi/2$ radians, previously multiplied by the complementary of $M_3(x, y)$, that are also added to $\alpha_M(x, y)$ before sending it to the SLM. The interferograms are formed after recombining both the light coming from the eliminated pixel-cells (reference beam) and the light modulated by the SLM at the remaining pixel-cells (object beam). The main advance of this procedure is that there is no need of extra optical elements (such as polarizers) to obtain the interferograms. However, this is done at the expense of a loss of resolution of the retrieved images because now the filtering process is more severe. That is, the filtering condition should be accommodated to the period of $M_3(x, y)$ instead of that corresponding to $M_1(x, y)$ or $M_2(x, y)$.

For this experiment, the amplitude and phase of the complex field are given by images of a young boy and girl, respectively [see Figs. 5(a) and 5(b)]. In addition, Figs. 5(c), 5(e), and 5(g) show the recovered amplitude images when employing binary gratings of 1×1 , 2×2 , and 5×5 pixels/cell, whereas the corresponding phase images are given in Figs. 5(d), 5(f), and 5(h).

From the experimental results shown in Fig. 5, one can confirm again that pixel cross-talk produces negative effects

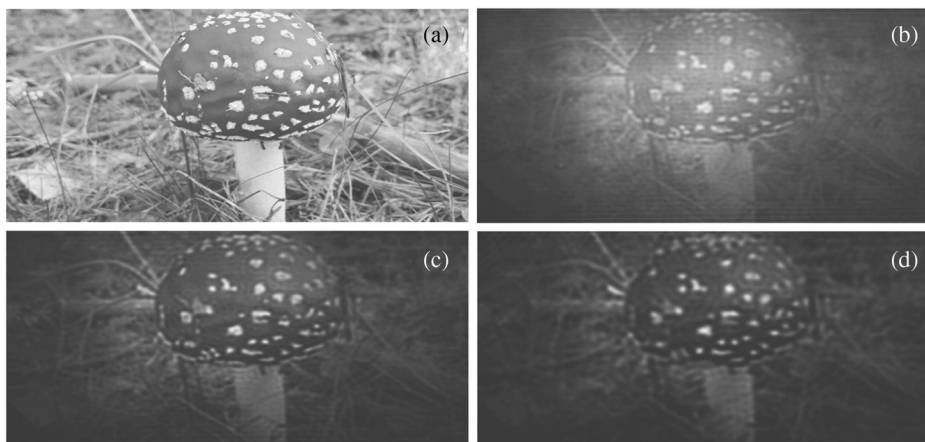


Fig. 3 (a) Original amplitude pattern and (b)–(d) the corresponding ones recorded with sampling gratings of 1×1 , 4×4 , and 10×10 pixels/cell, respectively.



Fig. 5 (a) Target amplitude and (b) phase images, and (c), (e), and (g) corresponding amplitude and (d), (f), and (h) phase images recorded for sampling gratings of 1×1 , 2×2 , and 5×5 pixels/cell, respectively.

in the quality of the recorded complex field. In particular, the contrast of amplitude patterns is clearly deteriorated when the pixel-cell size is decreased, whereas phase patterns seem to be poorly changed for the same reason. This last fact can be better understood if we rewrite the phase element as

$$\alpha(x, y) = \varphi(x, y) + \Theta(x, y), \quad (7)$$

where

$$\Theta(x, y) = M_1 \cos^{-1} \left[\frac{A(x, y)}{A_{\max}} \right] - M_2 \cos^{-1} \left[\frac{A(x, y)}{A_{\max}} \right]. \quad (8)$$

From Eqs. (7) and (8) one can realize that, in the double-phase method,²¹ the original phase $\varphi(x, y)$ is fully encoded into the SLM. In addition, the employed optical imaging system ensures a replica of $\varphi(x, y)$ at the output plane. So, any loss of resolution of phase images should be mainly caused by the filtering process. However, the term $\Theta(x, y)$ is directly related to the encoding of amplitude information, which can only be retrieved by means of the interference among nearby pixels. So, as the interference process strongly depends on the phase values of these pixels, the amplitude images are definitively more spoiled by the pixel cross-talk effects than phase ones. These conclusions were supported by the calculus of the root-mean-square error (RMSE) between the original and measured patterns. It yields RMSE of 23.5%, 21.6%,

and 19.5% for the amplitude patterns encoded with binary gratings of 1×1 , 2×2 , and 5×5 pixels/cells, respectively, whereas for the corresponding phase patterns, the numbers were 7.9%, 8.2%, and 9.1%, respectively.

4 Conclusions

In this paper, we have discussed and partially compensated for the effects of pixel cross-talk on the double-phase method²¹ implemented with phase-only PA-LCoS SLMs. Our experiments show that nonuniform phase modulation due to pixel cross-talk may deteriorate the quality of reconstructed images, which basically have less sharpness and contrast than expected. Hence, to mitigate unwanted cross-talk effects, we propose and experimentally demonstrate a generalized sampling scheme that preserves the accuracy of the double-phase method.²¹ We found that a slight increase of the grating's period beyond the Nyquist limit significantly reduces cross-talk effects. In addition, light efficiency should be also benefit from the better phase response of the liquid crystal display through the availability of more diffracted light. However, this always happens at the expense of decreasing the spatial resolution of the reconstructed hologram in the manner described by Eq. (6). In this paper, the measurements of the amplitude and phase patterns associated with the complex field were carried out with a convenient implementation of the polarization-based phase-shifting technique.³⁴

We believe that the results shown here can be useful for improving next experimental realizations of the double-phase method²¹ with phase-only PA-LCoS SLMs. At this point, it is apparent that the degree of damage in the reconstructed images should depend on the employed SLM and its technical specifications. That is why the selection of an optimum period for the binary gratings $M_1(x, y)$ and $M_2(x, y)$ can vary from one SLM to another, and it is clearly influenced by the final application.

Acknowledgments

The authors are also very grateful to the SCIC of the Universitat Jaume I for the use of the femtosecond laser. There are no conflicts of interest to declare.

References

- V. Arrizón, G. Méndez, and D. Sánchez-de-La-Llave, "Accurate encoding of arbitrary complex fields with amplitude-only liquid crystal spatial light modulators," *Opt. Express* **13**(20), 7913–7927 (2005).
- E. Ulusoy, L. Onural, and H. M. Ozaktas, "Full-complex amplitude modulation with binary spatial light modulators," *J. Opt. Soc. Am. A* **28**(11), 2310–2321 (2011).
- H. Songet et al., "Optimal synthesis of double-phase computer generated holograms using a phase-only spatial light modulator with grating filter," *Opt. Express* **20**(28), 29844–29853 (2012).
- S. Reichelt et al., "Full-range, complex spatial light modulator for real-time holography," *Opt. Lett.* **37**(11), 1955–1957 (2012).
- S. A. Goorden, J. Bertolotti, and A. P. Mosk, "Superpixel-based spatial amplitude and phase modulation using a digital micromirror device," *Opt. Express* **22**(15), 17999–18009 (2014).
- L. Zhu and J. Wang, "Arbitrary manipulation of spatial amplitude and phase using phase-only spatial light modulators," *Sci. Rep.* **4**, 7441 (2014).
- L. Wu, S. Cheng, and S. Tao, "Simultaneous shaping of amplitude and phase of light in the entire output plane with a phase-only hologram," *Sci. Rep.* **5**, 15426, (2015).
- T. W. Clark et al., "Comparison of beam generation techniques using a phase only spatial light modulator," *Opt. Express* **24**(6), 6249–6264 (2016).
- J. A. Davis et al., "Encoding amplitude information onto phase-only filters," *Appl. Opt.* **38**(23), 5004–5013 (1999).
- V. Arrizón et al., "Pixelated phase computer holograms for the accurate encoding of scalar complex fields," *J. Opt. Soc. Am. A* **24**(11), 3500–3507 (2007).
- T. Sarkadi, Á. Kettinger, and P. Koppa, "Spatial filters for complex wavefront modulation," *Appl. Opt.* **52**(22), 5449–5454 (2013).
- E. Bolduc et al., "Exact solution to simultaneous intensity and phase encryption with a single phase-only hologram," *Opt. Lett.* **38**(18), 3546–3549 (2013).
- T. Nobukawa and T. Nomura, "Linear phase encoding for holographic data storage with a single phase-only spatial light modulator," *Appl. Opt.* **55**(10), 2565–2573 (2016).
- J. L. Martínez-Fuentes and I. Moreno, "Random technique to encode complex valued holograms with on axis reconstruction onto phase-only displays," *Opt. Express* **26**(5), 5875–5893 (2018).
- C. Guo et al., "A fast-converging iterative method based on weighted feedback for multi-distance phase retrieval," *Sci. Rep.* **8**, 6436 (2018).
- M. A. Seldowitz, J. P. Allebach, and D. W. Sweeney, "Synthesis of digital holograms by direct binary search," *Appl. Opt.* **26**(14), 2788–2798 (1987).
- X. Li et al., "3D dynamic holographic display by modulating complex amplitude experimentally," *Opt. Express* **21**(18), 20577–20587 (2013).
- A. J. Cable et al., "Real-time binary hologram generation for high-quality video projection applications," in *SID Int. Symp. Digest Tech. Pap.*, Vol. 35, pp. 1431–1433 (2004).
- P. W. M. Tsang, Y.-T. Chow, and T.-C. Poon, "Generation of phase-only Fresnel hologram based on down-sampling," *Opt. Express* **22**(21), 25208–25214 (2014).
- P. W. M. Tsang, Y. T. Chow, and T.-C. Poon, "Generation of patterned-phase-only holograms (PPOHs)," *Opt. Express* **25**(8), 9088–9093 (2017).
- O. Mendoza-Yero, G. Mínguez-Vega, and J. Lancis, "Encoding complex fields by using a phase-only optical element," *Opt. Lett.* **39**(7), 1740–1743 (2014).
- J. Hu, C.-S. Brès, and C.-B. Huang, "Talbot effect on orbital angular momentum beams: azimuthal intensity repetition-rate multiplication," *Opt. Lett.* **43**(16), 4033–4036 (2018).
- Y. Qi, C. Chang, and J. Xia, "Speckleless holographic display by complex modulation based on double-phase method," *Opt. Express* **24**(26), 30368–30378 (2016).
- L. Gong et al., "Controllable light capsules employing modified Bessel-Gauss beams," *Sci. Rep.* **6**, 29001 (2016).
- C. Changet et al., "Shaping of optical vector beams in three dimensions," *Opt. Lett.* **42**(19), 3884–3887 (2017).
- T. Liet et al., "Multifocus autofocusing Airy beam," *J. Opt. Soc. Am. A* **34**(9), 1530–1534 (2017).
- Y. Zhaet et al., "Elliptical Airy beam," *Appl. Opt.* **57**(23), 6717–6720 (2018).
- A. Lizana et al., "Time fluctuations of the phase modulation in a liquid crystal on silicon display: characterization and effects in the diffractive optics," *Opt. Express* **16**(21), 16711–16722 (2008).
- J. L. Martínez et al., "Analysis of multiple internal reflections in a parallel aligned liquid crystal on silicon SLM," *Opt. Express* **22**(21), 25866–25879 (2014).
- S. Reichelt, "Spatially resolved phase-response calibration of liquid crystal-based spatial light modulators," *Appl. Opt.* **52**(12), 2610–2617 (2013).
- C. Lingel, T. Haist, and W. Osten, "Optimizing the diffraction efficiency of SLM-based holography with respect to the fringing field effect," *Appl. Opt.* **52**(28), 6877–6883 (2013).
- E. Ronzittiet et al., "LCoS nematic SLM characterization and modeling for diffraction efficiency optimization, zero and ghost orders suppression," *Opt. Express* **20**(16), 17843–17855 (2012).
- J. E. Stockley, D. Subacius, and S. A. Serati, "The influence of the inter-pixel region in liquid crystal diffraction gratings," *Proc. SPIE* **3635**, 1–10 (1999).
- I. Yamaguchi and T. Zhang, "Phase-shifting digital holography," *Opt. Lett.* **22**(16), 1268–1270 (1997).

Miguel Carbonell-Leal received his BS degree in computer engineering and MS degree in artificial intelligence from the University Jaume I (UJI), Spain, in 2014 and 2015, respectively. Since 2015, he has been working toward his PhD with the Photonics Group (GROC-UJI) at UJI. He is author of seven research papers and about 20 contributions to scientific congresses.

Omel Mendoza-Yero is a professor and researcher at the University Jaume I (UJI), Spain. He is a member of the Photonics Group (GROC-UJI) at UJI. He received his BS degree and PhD in physics from the University of Havana in 1998 and 2005, respectively. He is the author of more than 60 journal papers as well as several contributions to photonics congresses. His current research interests include ultrafast optics, diffractive optics, and beam shaping.